24th International Symposium on Dynamics of Vehicles on Roads and Tracks
IAVSD 2015, Graz, Austria, August 17-21, 2015 (Paper 17.1)

Modelling of rubber components using estimated parameters

O. Polach
Bombardier Transportation (Switzerland) AG, Winterthur, Switzerland

ABSTRACT: The aim of this paper is to compare different rubber component models used during the layout and preliminary vehicle engineering, when no components' measurements are available. The model parameter estimation is based on the component's static stiffness and on its dynamic stiffness at the estimated values of the main working frequency and amplitude. Six rubber component models are compared and their performance evaluated. Particular attention is dedicated to equivalent models consisting of a spring with multiple Maxwell elements in parallel. A method for parameter determination is proposed which provides suited results regarding the stiffening and loss energy and requires only 5 input values, independently of the number of Maxwell elements.

1 INTRODUCTION

Rubber components are widely used in railway vehicles. Several types of layered rubber-metal springs serve as a part of the suspension systems. Rubber bushes are used in the wheelset guidance systems, traction rods, anti-roll devices, linkage mechanisms and damper joints.

The rubber components properties are characterised by a stiffness K and a loss angle δ which are defined as follows (see Figure 1):

$$K = \frac{F_{\max} - F_{\min}}{z_{\max} - z_{\min}} \tag{1}$$

$$\delta = \arcsin \frac{W_{loss}}{\frac{\pi}{4}\left(F_{\max} - F_{\min}\right)\left(z_{\max} - z_{\min}\right)} \tag{2}$$

with W_{loss} = loss energy (loss work), i.e. the area of the force-displacement loop.

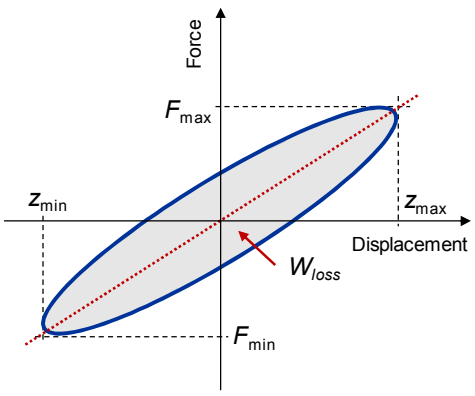

Figure 1. Identification of stiffness and los angle from a force-displacement diagram.

It is rather difficult to provide a general description of rubber components' properties in regard to frequency and amplitude. It is known that the dynamic stiffness is higher than the static one. The stiffness increases with increasing frequency, but there is also stiffness increase with decreasing displacement amplitude. A quantitative characterisation of dynamic stiffening is rather difficult because the publications presenting the stiffness data usually consider only certain type of component and certain range of frequencies and amplitudes. Eckwerth & Frohn [1] state that the frequency effect is dominant at frequencies approximately about 50 Hz, while the stiffness increase with a reduction of amplitude is particularly relevant at low frequencies. Even more difficult is to characterise the loss angle value. Some publications show an increase of the loss angle with increasing frequency, see e.g. Sjöberg & Kari (2002) [2]. The dependency of the loss angle on the amplitude is ambiguous; the loss angle remains often rather constant with the change of amplitude. Alonso et al. [3] present the loss angle results with a small maximum at an intermediate amplitude, more pronounced at the highest hardness of the tested rubber joint.

There are large number of investigations dealing with rubber modelling, see review papers [4] and [5]. The dynamic stiffening – an increase of stiffness with frequency compared to the static stiffness – can be modelled as a time relaxation force by parallel combination of a spring with a Maxwell element (ME), which is a dashpot with a spring in series. The stiffening related to small amplitudes can be modelled by a friction force in parallel to the elastic force. However, a simple Coulomb friction provides force-displacement diagrams differing from typical rubber measurement results. Therefore, specific friction models representing rubber hysteresis were developed, e.g. by Berg [6, 7] or by Pfeffer & Hofer [8].

Advanced rubber models contain besides elastic force both the time relaxation force and the friction force. Large application found the rubber model by Berg [6, 7], which uses friction described by a fractional expression. This friction model is combined in parallel with a spring and ME. A comprehensive investigation and comparison of equivalent rubber component models was presented by Sedlaczek et al. [9]. The model consists of three different branches: elastic, amplitude dependent and frequency dependent branch. The amplitude dependency is represented by a mathematical shape function based on Berg's approach. The frequency dependent branch uses either a set of two parallel MEs or a fractional differentiation, respectively, both options in combination with a dashpot in parallel. Yarmohamadi and Berbyuk [10] also use a model based on the superposition of elastic, viscous (2 MEs in parallel) and friction forces (Berg's friction model). In total seven model parameters are determined in a way to reduce the error between the measured and simulated stiffness and damping of a rubber mount. Other models and parameter identification procedures based on measured data are presented e.g. by Kim et al. [11], Zhang et al. [12] and Kaldas et al. [13].

The literature review demonstrates the need of measurement results to derive the parameters of advanced rubber component models. However, especially during the vehicle development, the components' measurements are not available. The engineers use the values in the component specification or the results of the calculations from the supplier.

In contrast to a number of other publications dealing with the models which intend to reproduce the available component measurements, this paper deals with a typical situation during the product development, when there are no component measurements available for layout and preliminary calculations. The aim of this paper is to compare different rubber component models and to provide recommendations for the estimation of their parameters. The possible modelling options are compared and advantages and limitations of different models discussed.

2 ASSUMPTIONS USED FOR THE PARAMETER ESTIMATION

The aim of the presented investigations is to compare the rubber component models which allow representation of the vehicle behaviour regarding dynamic as well as quasi-static conditions with one parameter set. Although the dynamic stiffening is related not only to frequency but also to amplitude, a pure frequency dependent modelling of the stiffening can be acceptable because of typical relationship between the frequencies and amplitudes. When running on tracks with stochastic irregularities, the amplitudes of displacements are reduced with increasing frequency. To allow a comparison of different models representing the dependency either on fre-

quency or on amplitude, we assume in some comparisons that the product P of a frequency f and an amplitude A will remain constant. The amplitude A is then

$$A = \frac{P}{f} \qquad f > 0 \text{ Hz} \tag{3}$$

The proposed parameter estimation of a rubber component model is based on the estimated or on the requested (specified) component's performance. This is a typical situation during rolling stock development, when component measurements are not available. The parameters used as input data are:

- static component stiffness K_{st}
- dynamic component stiffness K_n and loss angle δ_n (or relative damping D_n, respectively) for the main working point in vehicle service, i.e. the typical frequency f_n, and amplitude A_n (called also nominal or maim working frequency and amplitude).

The typical working frequency can be represented e.g. by a bouncing of car body for rubber secondary springs (either regular or emergency springs), a frequency of bogie bouncing for rubber primary springs, or a hunting frequency regarding wheelset guidance bushings, respectively.

The most widely used rubber component's model is a spring with stiffness k and a dashpot with damping rate c in parallel, called Kelvin-Voigt element. Let us first discuss the determination of parameters of this model. We consider a harmonic excitation with an angular frequency ω and an amplitude z_{max}

$$z(i\omega) = z_{\max} e^{i\omega t} \tag{4}$$

The force on the Kelvin-Voigt element is

$$F(i\omega) = (k + i\omega c) z_{\max} e^{i\omega t} \tag{5}$$

and the complex stiffness yields

$$K(i\omega) = \frac{F(i\omega)}{z(i\omega)} = k + i\omega c \tag{6}$$

The maximum component force is a vector sum of the real component $F_{\max \mathrm{Re}}$ and the imaginary component $F_{\max \mathrm{Im}}$

$$F_{\max\ \mathrm{Re}} = k z_{\max}, \quad F_{\max\ \mathrm{Im}} = c\omega z_{\max} \tag{7}$$

The magnitude of the complex stiffness $K(i\omega)$ is then

$$K = \frac{F_{\max}}{z_{\max}} = \sqrt{k^2 + (\omega c)^2} \tag{8}$$

As the Kelvin-Voigt element cannot represent the typical difference between the static and dynamic stiffness of rubber components as known from railway practice, the determination of model parameters is based on the dynamic stiffness K_n and on the damping performance, characterised either by a loss angle δ_n or a relative damping D_n of the oscillating system, respectively. The spring stiffness k of the Kelvin-Voigt element is set equal to the target stiffness K_n. The estimation of the dashpot damping rate c can be provided based on an equivalent mass-spring system with a mass m connected to ground by the Kelvin-Voigt element. This mass-spring system with the eigenfrequency f_n represents the behaviour of the investigated system. The relative system damping D (defined as system damping related to the critical damping) is

$$D = \frac{c}{c_k} = \frac{c\omega_n}{2k} = \frac{c\pi f_n}{k} \tag{9}$$

with ω_n = nominal angular frequency.

If the relative damping D_n is used as an input value, we receive the dashpot's damping rate c from Equation (9). Alternatively, when using the loss angle δ_n as an input value, this formula can be modified using the relationship between the loss angle δ and the relative damping D

$$D = \frac{1}{2}\tan\delta \tag{10}$$

The damping rate c of the dashpot yields then

$$c = \frac{kD_n}{\pi f_n} = \frac{k}{2\pi f_n}\tan\delta_n \tag{11}$$

This parameter estimation method can be applied also to other models consisting of linear elements (i.e. springs and dashpots) by transforming them to an equivalent Kelvin-Voigt model with the complex stiffness

$$K(i\omega) = K_e + i\omega\, C_e \tag{12}$$

with K_e, C_e representing an equivalent stiffness or damping, respectively, of a Kelvin-Voigt element which has the same behaviour as the investigated model.

3 A COMPARISON OF COMMON RUBBER COMPONENT MODELS

A comparison of 6 different model types was conducted in the framework of an EU-founded research project DynoTRAIN [14]. Each model consists of a spring, which can be either linear or nonlinear, in parallel with other force element(s) as a dashpot, a Maxwell element, or a friction element according to Berg, see Figure 2.

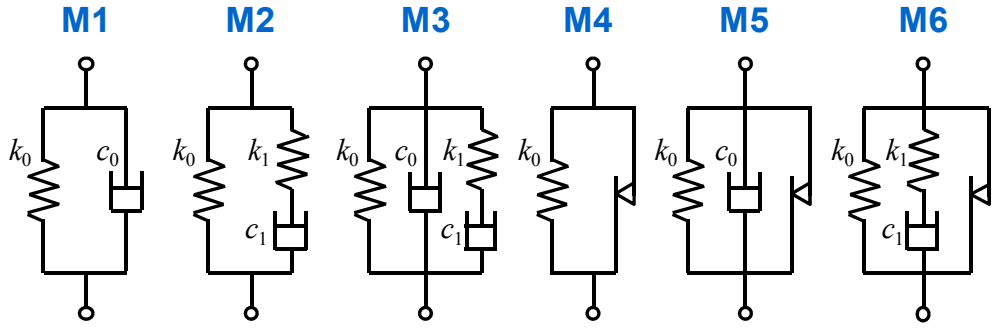

Figure 2. Compared models of rubber components.

The following data are considered as input in the presented examples:

- Static stiffness K_{st} = 3 kN/mm
- Main working point with frequency f_n = 4 Hz and amplitude A_n = 2 mm
- Dynamic stiffness K_n = 4.2 kN/mm at the frequency f_n and amplitude A_n
- Relative damping D_n = 5% (or, alternatively using Equation 10, a loss angle of δ_n = 5.7°) at the frequency f_n and amplitude A_n.

This input data represents a stiffness increase of 40% between the static and the dynamic stiffness. This rather high value of dynamic stiffening was selected to test the modelling options using a challenging example. For a sake of brevity, only the case with a linear stiffness k_0 of the spring in the left part of each model is considered in the presented examples.

The model M1 does not allow fulfilment of both target values of static and dynamic stiffness. The spring stiffness k_0 is thus set to the dynamic stiffness K_n and the dashpot's damping rate c_0 is determined to achieve the target damping performance as shown in Chapter 2. All other models allow the representation of dynamic stiffening. Thus, the elastic force of the spring k_0 is defined by the static stiffness K_{st} and the model parameters are determined with the aim to fulfil the target dynamic stiffness K_n and the target loss angle δ_n (or the target relative damping D_n, respectively) in the main working point.

The main differences between the behaviour of the models are visualised in Figure 3, which displays the stiffness and the loss angle diagrams of models M1, M2, M4 and M6. The static

stiffness of the model M1 is the same as the target dynamic stiffness. The model M2 represents only a stiffness dependency on frequency, whereas the stiffness of model M4 depends only on amplitude. The stiffness dependency on both amplitude and frequency can be seen only with the model M6. The loss angle of the model M1 increases unrealistically strongly with frequency, whereas it decreases for M2 after an intermediate maximum at a frequency slightly higher than zero. The models M4 and M6 show similar loss angle results; rather constant, only slightly dependent on amplitude.

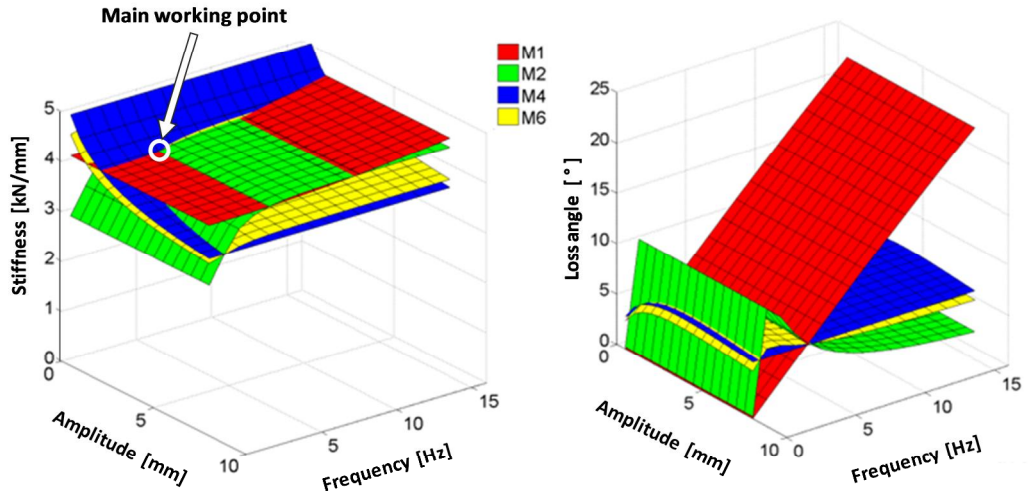

Figure 3. Comparison of models M1, M2, M4 and M6: Stiffness (left) and loss angle (right) in dependency of frequency and amplitude.

A comparison of stiffness and loss angle results for all compared models can be seen in Figure 4. The model M2 represents the dynamic stiffening by the visco-elastic force of ME. Applying the same dashpot damping rate $c_1 = c_0$ as in the model M1, the loss angle would be too high. To reduce the loss angle, we have to select a higher damping rate c_1 which results in a lower break frequency of ME. The target loss angle in the main working point is fulfilled selecting model parameters with a break frequency of 1.4 Hz. However, the loss angle is large at low frequencies, while vanishing at higher frequencies.

The model M3 possesses an additional dashpot c_0, so that the damping will not go down to zero at high frequencies. Using the damping rate c_0 close to the value used in the model M1, we get a break frequency of 0.5 Hz. The target loss angle in the main working point is fulfilled and increases with frequency above the main working point.

The friction element of model M4 is selected to fit to the loss energy at the nominal frequency f_n. The loss energy of model M5 is provided not only by the friction element but also by the dashpot. Because the target loss energy can be achieved by an arbitrary combination of both effects, one has to estimate the spread between them. As the presented comparisons concentrate on rather low frequencies, we consider that the viscous damping contributes to loss energy by 20% and the friction damping by 80%.

The model M6 is the model by Berg [6, 7]. To estimate the parameters of this model, one have to assume the distribution of the loss energy between the viscous and the friction damping and also the break frequency of ME. The parameter estimation thus requires a good experience. We selected parameters resulting in a break frequency of 1.45 Hz (i.e. close to the break frequency of the model M2) and a distribution of the loss energy between the viscous and the friction damping similar to the model M5.

To allow a better comparison of linear and nonlinear models, Figure 5 shows results considering a constant product of amplitude and frequency of $P = 8$ mmHz. All models besides M1 show an increase between the static and dynamic stiffness values, but the dynamic stiffening is higher at the models with friction (M4, M5, M6). However, there are large differences in the loss angle results.

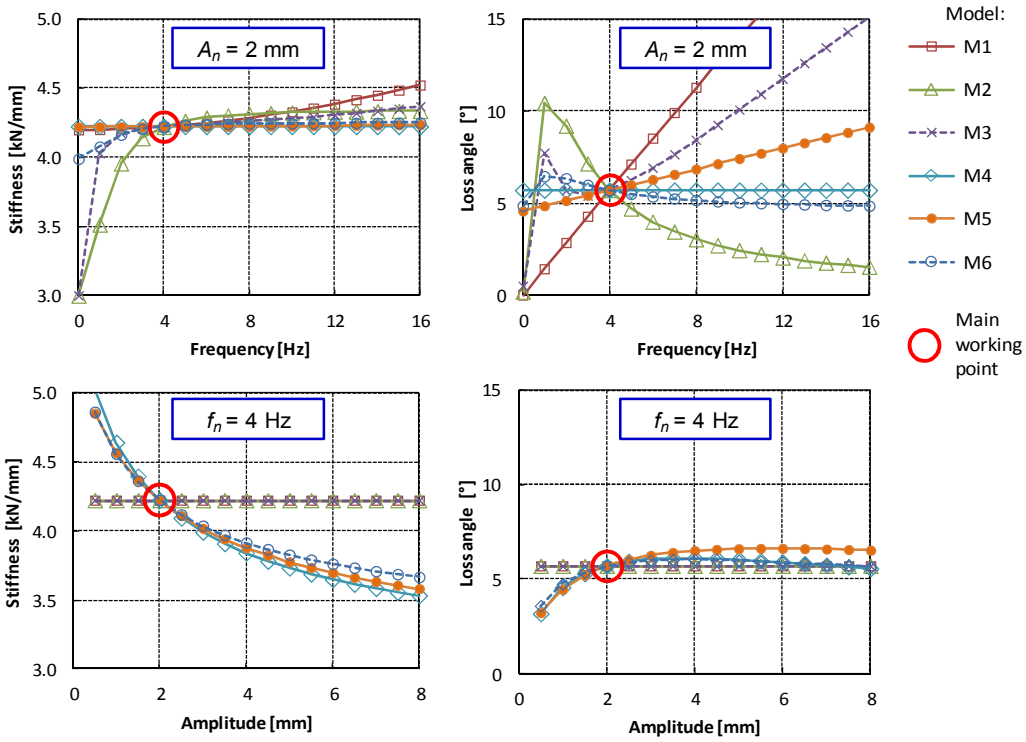

Figure 4. Comparison of all models: Stiffness (left) and loss angle (right) in dependency of frequency (top) and amplitude (bottom).

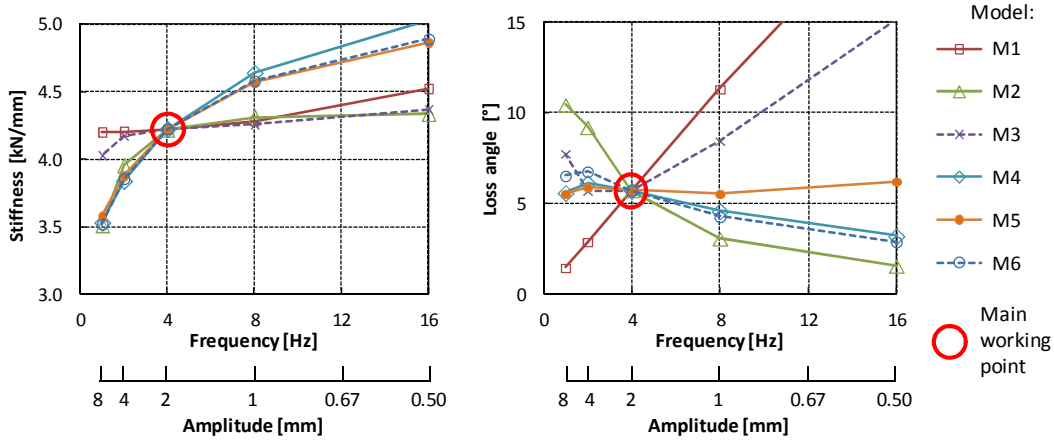

Figure 5. Stiffness and loss angle of the compared models assuming a constant value of the product of frequency and amplitude.

4 MODIFICATIONS OF LINEAR RUBBER MODELS AND THEIR LIMITATIONS

The parameters of models consisting of linear elements show only a frequency dependent performance. They however can be applied to model the dynamic stiffening of rubber components considering that the amplitude decreases with an increasing frequency. The advantage of this modelling is not only its possible application in linearised calculations but also an easier determination of suited model parameters to represent the dynamic stiffening of a rubber component.

The parameters of the models consisting of linear elements presented in Chapter 3 were identified by an iterative process comparing the stiffness and the loss energy at the main working frequency. The following presentation will derive the formulae for the parameter determination and discuss the performance of these models.

The model M2 is represented by 4 input values. Three of them are: Static stiffness K_{st} , frequency f_n of the main (typical) working point and dynamic stiffness K_n at the frequency f_n . The fourth input value can be either the loss angle δ_n at the nominal frequency f_n, or the maximum stiffness $K_{\max}$ at infinite frequency, or the break frequency f_b of ME

$$f_b = \frac{1}{2\pi}\frac{k_1}{c_1} \tag{13}$$

The component's stiffness will stay in the range of k_0 and (k_0 + k_1) and monotonically increase with excitation frequency, reaching its maximum value at the infinite frequency. The spring stiffness k_0 is equal to the static stiffness K_{st}.

Using the break frequency f_b as input, the dashpot damping rate c_1 can be expressed by Equation (13). The determination of the real part F_{Re} and the imaginary part F_{Im} of the elastic and damping forces at the main working frequency f_n yields in a quadratic equation of parameter k_1

$$k_1^2 + 2k_0k_1 + \left(k_0^{\,2} - K_n^2\right)\frac{f_b^2 + f_n^{\,2}}{f_n^{\,2}} = 0 \tag{14}$$

The positive solution of this quadratic equation provides the stiffness k_1

$$k_1 = -k_0 + \sqrt{k_0^{\,2} - \left(k_0^{\,2} - K_n^{\,2}\right)\frac{f_b^2 + f_n^{\,2}}{f_n^{\,2}}} \tag{15}$$

The damping rate c_1 is determined using Equation (13)

$$c_1 = \frac{1}{2\pi}\frac{k_1}{f_b} \tag{16}$$

The stiffness and loss angle in function of frequency for break frequencies f_b between 0.5 and 8 Hz are displayed in Figure 6. Dependent on the selected break frequency, there can be either nearby no increase of the stiffness above the main working frequency f_n, or a stiffness increase which is spread over a large frequency range and provides the maximum stiffness $K_{\max}$ of more than twice of the static stiffness. Both targets – the stiffness K_n as well the loss angle δ_n – are fulfilled for a break frequency of 1.43 Hz. The stiffness and the loss angle curves for this input data are included in Figure 6. One can observe that the loss angle curve is first increasing but then falling down with increasing frequency. The loss angle values are very low at high frequencies. This is in contrast with typical measurements showing rather marginal change of the loss angle with frequency.

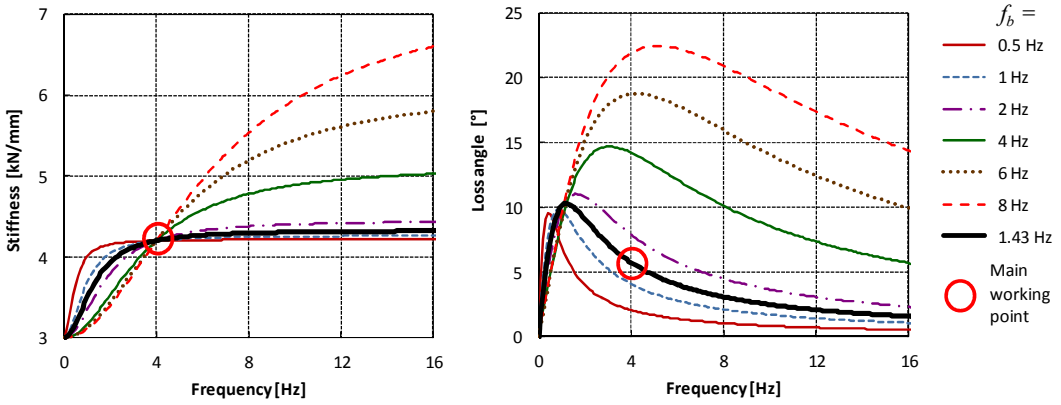

Figure 6. Stiffness and loss angle of the model M2 for different break frequencies.

To get an equivalent model with a stiffening distributed over a larger frequency range and a rather constant loss angle, the models M2 or M3 need to be extended with additional MEs in parallel. For the sake of brevity, we will neglect the dashpot in parallel as used in the model M3; the following investigations thus represent an extension of the model M2.

The nomenclature of the investigated model with multiple MEs is shown in Figure 7. This model is defined by $(1+2n_M)$ parameters, with n_M = number of MEs.

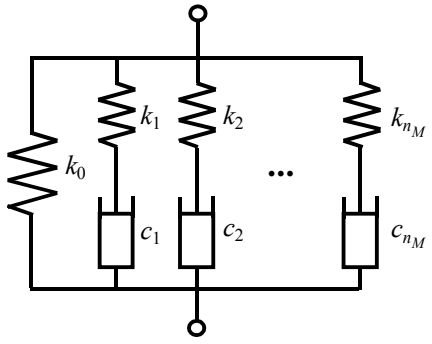

Figure 7. Model M2 extended to n_M Maxwell elements.

The selection of break frequency of the i-th ME for a stiffness increase in the range between a low frequency f_l and a high frequency f_h is proposed according to the following equation (based on a proposal presented in [15])

$$f_{b_i} = \frac{1}{2}\left\{10^{\left[\log f_l + (\log f_h - \log f_l)\frac{i-1}{n_M}\right]} + 10^{\left[\log f_l + (\log f_h - \log f_l)\frac{i}{n_M}\right]}\right\} \tag{17}$$

The series stiffness of MEs should decrease with increasing break frequency to avoid a too large relative damping. The following distribution of series stiffness k_i is proposed using a function with parameter α:

$$k_i = \alpha^{(n_M - i)} \frac{K_{\max} - K_{st}}{\sum_{i=1}^{n_M} \alpha^{(i-1)}} \tag{18}$$

The dashpot damping rate of the i-th ME is

$$c_i = \frac{k_i}{2\pi f_{b_i}} \tag{19}$$

The elastic and damping component's forces yield

$$F_{\max \mathrm{Re}} = \left[k_0 + \sum_{i=1}^{n_M} \frac{k_i \left(\frac{f_n}{f_{b_i}}\right)^2}{1 + \left(\frac{f_n}{f_{b_i}}\right)^2}\right] z_{\max}, \quad F_{\max \mathrm{Im}} = \left[\sum_{i=1}^{n_M} \frac{c_i}{1 + \left(\frac{f_n}{f_{b_i}}\right)^2}\right] \omega z_{\max} \tag{20}$$

and the stiffness K_n is

$$K_n = \frac{F_{\max}}{z_{\max}} = \frac{1}{z_{\max}} \sqrt{F_{\max \mathrm{Re}}{}^2 + F_{\max \mathrm{Im}}{}^2} \tag{21}$$

The model parameters can be determined numerically by varying the parameter α in Equation (18) with the aim to achieve the target stiffness value K_n.

To reduce the number of the input values to be estimated, the low frequency f_l can be set as a function of the selected high frequency f_h. The following function was evaluated to provide suited results

$$f_l = \frac{n_M f_h}{\log(n_M - 1)} \tag{22}$$

The loss angle (or the relative damping) at the main working frequency f_n is determined by other target values and is thus not used as input. It can be used as a target value instead of one of the previous target values; however, the solution exists only for some input data sets.

This methodology allows a reduction of the total number of input values to 5, independently of the number of MEs. The results for the models with 1 ME, 3 MEs and 5 MEs are shown in Figure 8 and compared with the nonlinear model by Berg considering that the amplitude A depends on frequency f according to Equation (3) with P = 8 mmHz. The model with 3 MEs provides the best agreement with the Berg's model regarding the stiffening; however, the loss angle is higher than the target value. The model with 5 MEs shows approximately constant value of the loss angle in the investigated frequency range, with values close to the Berg's model.

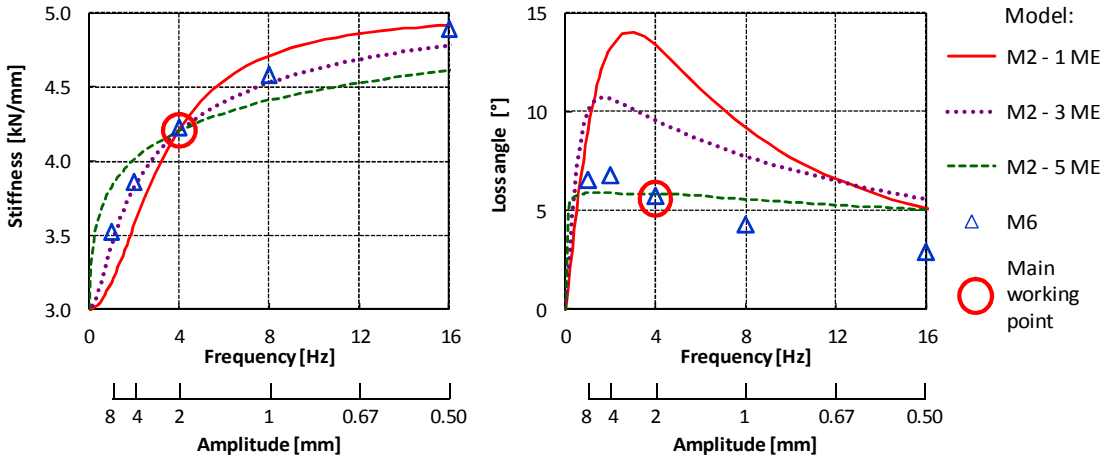

Figure 8. Stiffness and loss angle of the model M2 extended to 3 or 5 Maxwell elements, respectively, in comparison with nonlinear model M6 by Berg.

5 SUMMARY AND CONCLUSIONS

Rubber components are widely used in modern railway vehicles. Simulation models used in running dynamics have to represent at least approximately the properties of rubber components, particularly the dynamic stiffening. However, the measurements suited for identification of model parameters are often not available, mainly during the layout and preliminary engineering phases. This paper deals with this situation. Different rubber component models are compared and recommendations for the estimation of their parameters provided.

The stiffness of rubber components shows dependency on amplitude as well as on frequency. The modelling of a stiffness increase at smaller amplitudes requires application of a friction element, preferably a friction model suited to represent the hysteresis loop typical for rubber components. Nevertheless, the dynamic stiffening can be modelled also using models consisting of linear components, assuming that the amplitude reduces with an increasing frequency, which is a typical relationship when running on stochastic track irregularities. To consider this effect, we assume that the product of frequency and amplitude remains constant. On this way, the stiffening dependent on the amplitude and on the frequency can be represented by a frequency dependent behaviour only, which can be modelled using linear elements.

Using a model with one ME only, one can modify the break frequency of ME and the maximum dynamic component's stiffness to achieve the required stiffness at the main working point. Such model, however, often provides a too large loss energy, unless the dynamic stiffening is limited to a small frequency range. Using more than one ME in parallel, the stiffening is spread over a wider range of frequencies and the loss angle remains rather constant in larger frequency range. A method for parameter determination of models with multiple MEs is proposed. This method requires only 5 input values independently of the number of MEs and provides suited results regarding the stiffening and loss angle.

ACKNOWLEDGEMENT

The comparison of rubber models presented in Chapter 3 was undertaken in the context of the DynoTRAIN project, a medium-scale focused research project supported by the European 7th Framework Programme, contract number: 234079. I would like to thank my former colleague Patrick Renggli for his contribution as well as other project partners for their feedback during the project meetings.

REFERENCES

[1] Eckwerth, P, Frohn, J: Elastische Lagerungen in der Verkehrstechnik (in German). *ZEVrail Glasers Annalen* 128 (2004), No. 1-2, pp. 48-57

[2] Sjöberg M, Kari, L: Non-linear behavior of a rubber isolator system using fractional derivatives. *Vehicle System Dynamics* 37 (2002), No. 3, pp. 217-236

[3] Alonso A, Gil-Negrete N, Nieto J, Gimenez JG: Development of a rubber component model suitable for being implemented in railway dynamic simulation programs. *Journal of Sound and Vibration* 332(2013), pp. 3032–3048

[4] Eickhoff BM, Evans JR, Minnis AJ: A review of modelling methods for railway vehicle suspension components, *Vehicle System Dynamics* 24 (1995), pp. 469-496.

[5] Bruni S, Vinolas J, Berg M, Polach O, Stichel S: Modelling of suspension components in rail vehicle dynamics context. *Vehicle System Dynamics* 49 (2011), pp. 1021-1072

[6] Berg M: A model for rubber springs in the dynamic analysis of rail vehicles. *Proc. Instn. Mech. Engrs., Part F, Journal of Rail and Rapid Transit* 211 (1997), pp. 95-108

[7] Berg M: A non-linear rubber spring model for rail vehicle dynamics analysis. *Vehicle System Dynamics* 30 (1998), pp. 197-212

[8] Pfeffer P, Hofer K: Einfaches nichtlineares Modell für Elastomer- und Hydrolager zur Optimierung der Gesamtfahrzeug-Simulation (in German). *ATZ* 104 (2002), No. 5, pp. 442-451

[9] Sedlaczek K, Dronka S, Rauh J: Advanced modular modelling of rubber bushings for vehicle simulations. *Vehicle System Dynamics* 49 (2011), pp. 741–759

[10] Yarmohamadi H, Berbyuk V: Computational model of conventional engine mounts for commercial vehicles: validation and application. *Vehicle System Dynamics* 49 (2011), pp. 761–787

[11] Kim HJ, Yoo WS, Ok JK, Kang DW: Parameter identification of damping models in multibody dynamic simulation of mechanical systems. *Multibody System Dynamics* 22 (2009), pp. 383–398

[12] Zhang L, Yu Z, Yu Z: Novel empirical model of rubber bushing in automotive suspension system. *Proceedings of the ISMA2010-USD2010 Conference*, Katholieke Universiteit Leuven, Belgium, 20-22 September 2010, pp. 4259-4274

[13] Kaldas M, Caliskan K, Henze R, Kücükay F: Non-parametric modelling of damper top mounts. *Proc. Instn. Mech. Engrs. Part D: J Automobile Engineering* 226 (2012), No. 6, pp. 740–753

[14] Web: http://www.triotrain.eu (assessed 19.6.2015, 18:30)

[15] Cosco FI, Gatti G, Toso A, Donders S, Mundo D: An optimized identification method for modular models of rubber bushings. In: *RASD 2013 11th International Conference*, 1-3 July 2013, Pisa, Italy